

THE INVESTIGATION OF AN Al7075 ALLOY PREPARED BY SPARK PLASMA SINTERING OF MILLED POWDERS

MOLNÁROVÁ Orsolya^{1*}, MÁLEK Přemysl¹, NÉMETH Gergely¹, KOZLÍK Jirí¹, LUKÁČ František², CHRÁSKA Tomáš², CINERT Jakub²

¹Charles University in Prague, Czech Republic, EU, [*mopersze@gmail.com](mailto:mopersze@gmail.com)

²Institute of Plasma Physics of the CAS, Prague, Czech Republic, EU

Abstract

Atomized powder of an Al7075 alloy was high energy ball milled at room and cryogenic temperatures and compacted by spark plasma sintering (SPS) method. The influence of processing parameters on phase composition and microstructure was studied by X-ray diffraction, light and scanning electron microscopy. The mechanical properties were characterized by microhardness measurements.

The atomized powder contained a large volume fraction of intermetallic phases located predominantly in continuous layers separating cells or dendrites in the interior of individual powder particles. Consolidation by SPS destroyed partially this morphology and replaced it by individual particles located at boundaries of original powder particles, at cell boundaries or arranged in chains in previous dendritic regions.

High energy milling destroyed most intermetallic particles and enriched the matrix by solute atoms. The high deformation energy introduced into the powder during milling enhanced microhardness up to 220 HV. Consolidation of milled powders by SPS led to the formation of very fine-grained structure with the grain size even below 1 μm and with the fraction of high-angle boundaries about 0.9. Two main types of heterogeneously distributed precipitates were found. The irregularly shaped precipitates with a size about 1 μm seemed to encompass areas with rod like nano-precipitates in most samples. A drop in microhardness to 118HV was observed after SPS, predominantly due to a release of introduced deformation energy.

Keywords: Milling, cryo-milling, spark plasma sintering, ultrafine-grained materials

1. INTRODUCTION

Ultrafine-grained (UFG) materials exhibit generally a unique microstructure and excellent mechanical properties, e.g. enhanced strength [1, 2]. Grain refinement can be achieved by a wide variety of producing methods (recrystallization, severe plastic deformation, rapid solidification etc.). Powder metallurgy deserves a special attention among them [2, 3].

The powders can be produced by gas atomization process. The microstructure of gas atomized powder particles is frequently very fine and their phase composition is far from equilibrium [3]. This deviation from equilibrium increases with increasing solidification rate, i.e. with decreasing size of powder particles. In case of a broad distribution of powders size, a variety of microstructures can be observed [4]. The atomized powder can be subjected to high energy milling which introduces large deformation energy into the powder particles and enhances further the strength [3].

To prepare bulk material from atomized or milled powders a suitable consolidation method has to be chosen. The main goal is to preserve the excellent microstructure and strength during sintering. Spark plasma sintering (SPS) is a modern technique combining concurrent uniaxial pressure and direct heating by a pulsed DC current [5]. Comparing to other consolidation methods, SPS enables sintering at lower temperatures and in shorter time. The high heating rate and short thermal exposure help to minimize undesirable processes like recrystallization or grain growth and therefore helps to preserve the powders fine-grained structure [5].

The high strength Al7075 aluminum alloy is widely used in transportation and construction industry. Its strength is deduced preferentially from precipitation strengthening, however, fine grain size can further improve its properties. The aim of this study was to verify the possibility of producing high strength UFG material by powder metallurgy. The gas atomization, high energy milling at room or cryogenic temperatures and following spark plasma sintering was used. The influence of processing parameters on the microstructure, phase composition and microhardness was investigated.

2. EXPERIMENTAL

The nitrogen atomized Al7075 powder supplied by Nanoval GmbH & Co. KG, Berlin was sieved down to 50 μm . The resulting average powder particle size was 23 μm . The alloy composition is given in **Table 1**.

Table 1 The alloy composition

	Zn	Mg	Cu	Fe	Ti	Al
wt. %	6.15	2.73	1.68	0.07	0.02	Balance

The atomized powder was milled in an UNION HD01 Lab Attritor using stainless steel balls (ball to powder ratio of 32:1) either at room temperature (RT) in Ar gas or at cryo-temperature in liquid nitrogen. During milling at RT the tank jacket was cooled by water stream. The milling parameters are listed in **Table 2**.

Table 2 The notation of samples, frequency RPM (revolutions per minute), milling time t , milling media

Material	A	RT_180x3	RT_400x3	RT_400x8	cryo_180x3	cryo_400x3
RPM (min^{-1})	atomized	180	400	400	180	400
t (h)		3	3	8	3	3
Milling media		Ar gas	Ar gas	Ar gas	liquid N	liquid N

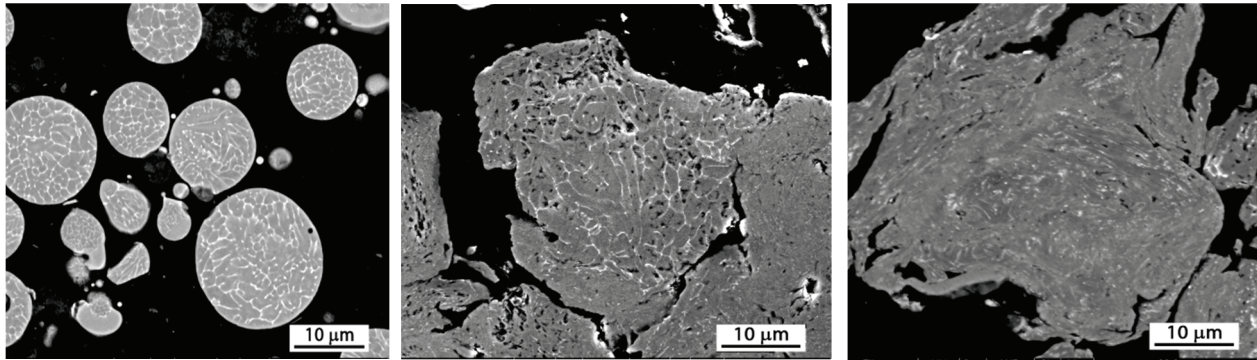
The X-ray diffraction (XRD) measurements were carried out on vertical θ - θ diffractometer D8 Discover (Bruker AXS, Germany) equipped with divergent beam optics using $\text{CuK}\alpha$ radiation. Diffracted beam was detected by 1D detector LynxEye. Phase identification was done using Diffrac. Eva with accessed PDF-2 database of crystalline phases. Quantitative Rietveld refinement was performed in TOPAS V5, aiming at determination of wt.% of all the identified phases following the theory from [6, 7].

Light microscopy (LM) was performed using Olympus IX70 microscope on cold mounted powders or on metallographically processed compacts. Dix-Keller reagent was used to reveal the microstructure. For scanning electron microscopy (SEM) in backscattered electron (BSE) imaging mode and for electron backscatter diffraction (EBSD), the powders were hot mounted (180 $^{\circ}\text{C}$, 2.5 min) by conductive resin with carbon filler. The samples from SPS compacts were cut parallel to the pressure direction in SPS. The sample preparation included mechanical grinding, polishing and electrolytic polishing (just in case of EBSD measurements). SEM and energy dispersive X-ray spectroscopy (EDS) analysis were completed by FEI Quanta 200F, equipped by EDAX Trident. DigiView 3 camera from company EDAX with OIM software was employed for EBSD.

Microhardness measurements were carried out on polished samples using a microhardness tester Qness Q10A+ equipped with a Vickers indenter. The load between 1 and 10 g was applied at powder material depending on the microhardness of the investigated powder samples. At least 15 different powder particles were measured. A load of 50 g was applied in case of compact samples. To study the materials homogeneity an area of 4x4 mm^2 was tested automatically with a distance between indents of 200 μm .

3. RESULTS

Figure 1 shows the SEM micrographs documenting the microstructural evolution due to milling.



a) Atomized powder particles b) RT_180x3 powder particles c) cryo_180x3 powder particles

Figure 1 The SEM/BSE micrographs of atomized and milled powder particles

The atomized powder contains mostly spherical particles. Their microstructure is formed either by equiaxed and columnar cells or dendrites divided by continuous layers of intermetallic particles. According to XRD measurements, $MgZn_2$ is present in the atomized powder. Both LM and SEM investigations revealed that already milling at 180 RPM for 3 h altered the powders structure. The particle size was increased and their irregular shape reflected repeated fracture and cold welding of particles during milling. Some former cells are still recognisable in the particle microstructure, but they are deformed or even destroyed. With increasing intensity of milling (increasing milling rate and time or decreasing milling temperature) the microstructure became fully destroyed and the particles porous. Milling also destroyed most intermetallic phases; only a very small amount of $MgZn_2$ was found (**Figure 2**). The content of $MgZn_2$ phase was found to decrease with decreasing temperature and increasing RPM of milling. Simultaneously a significant increase in materials microstrain was confirmed by XRD.

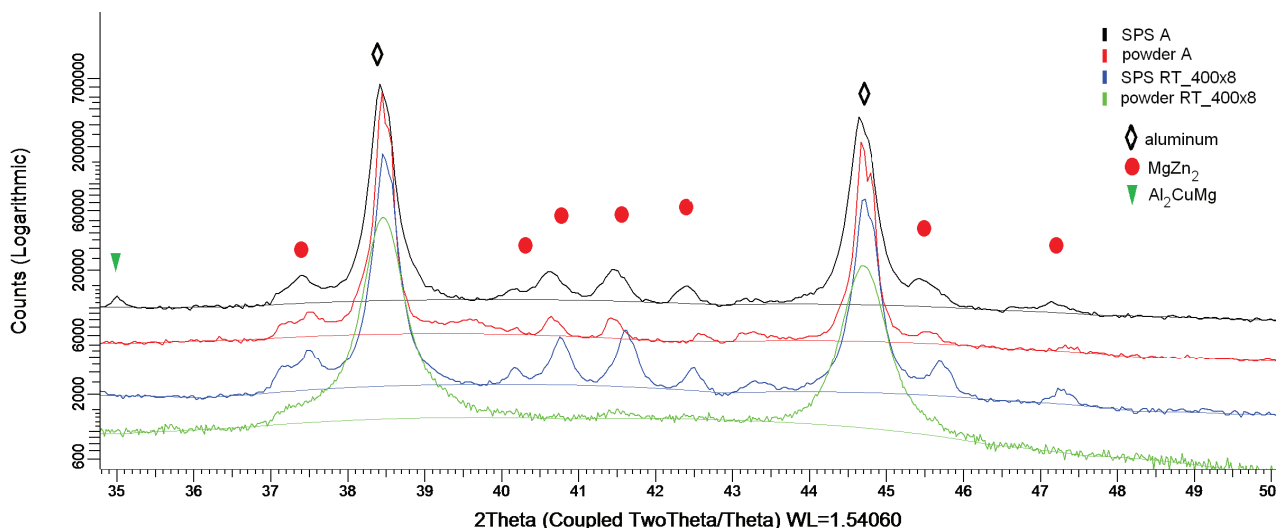
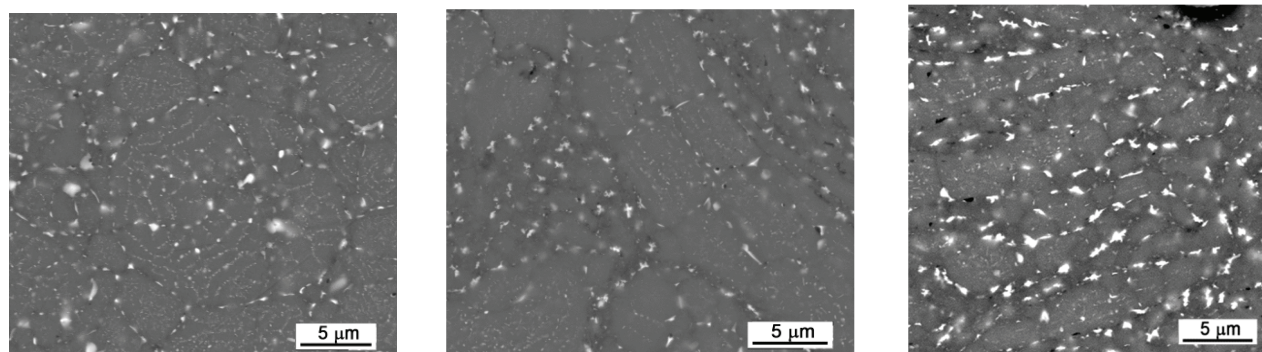


Figure 2 A part of the XRD pattern for a selected (RT_400x8) milled powder and its SPS compact, compared to the XRD pattern from atomised powder and its compact

The SPS process led to dense compacts. The continuous layers of intermetallic phases present in atomized powders were replaced predominantly by chain-like structures along former internal boundaries (**Figure 3a**). The particles were identified to be $MgZn_2$ and Al_2MgCu . **Figure 3b** shows a heterogeneous microstructure of

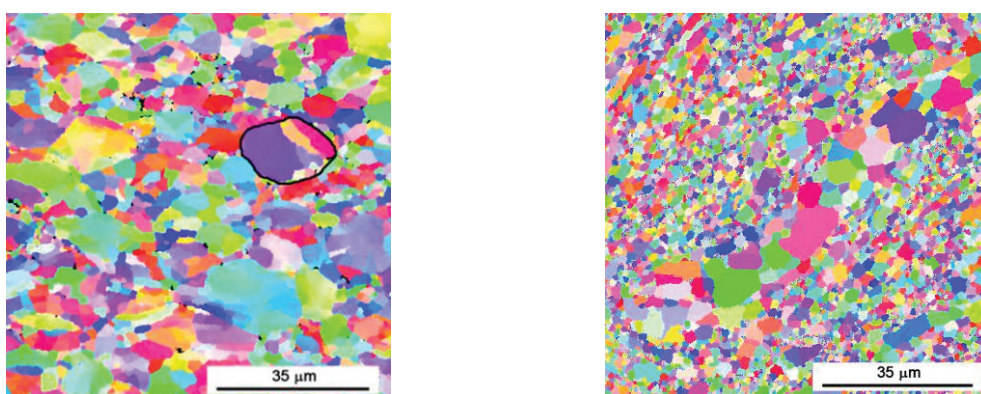
SPS compact prepared from a milled powder - the irregularly shaped precipitates (the size slightly below 1 μm) seem to form boundaries around areas with rod-like nanoparticles. Increasing intensity of milling reduced this heterogeneity (**Figure 3c**). The size and volume fraction of the MgZn_2 phase in SPS compacts increased with increasing intensity of milling. The SPS caused a slight increase of matrix crystallite size and a decrease in microstrain.



a) compact from atomized powder b) compact from RT_180x3 c) compact from cryo_180x3

Figure 3 The SEM/BSE micrographs of SPS compacts prepared from atomized and milled powders

Figure 4 compares the EBSD orientation maps of SPS compacts prepared from atomized and a selected (RT_400x3) milled powder. The original powder particles are still visible in the compact prepared from atomized powder, one is highlighted by black boundary (**Figure 4a**). The microstructure of the compact prepared from milled powders is much finer - the regions with ultrafine-grained microstructure are combined with coarser grains with the size up to 5 μm , predominantly high angle boundaries were observed.



a) EBSD micrograph of the atomized compact b) EBSD micrograph of RT_400x3 compact

Figure 4 The EBSD map of compacts from atomized and milled powders

Table 3 lists the average microhardness of different powders and compacts. The HV values were determined up to 3 h from the milling or SPS process to avoid the effect of rapid natural aging of the studied alloy [8]. The powders HV increased by intensity of milling. The SPS process caused a drop in HV in all materials.

Table 3 The microhardness of different powders and corresponding SPS compacts

Material	A	RT_180x3	RT_400x3	RT_400x8	cryo_180x3	cryo_400x3
HV powder	127 \pm 41	136 \pm 40	216 \pm 20	229 \pm 29	188 \pm 21	220 \pm 20
HV compact	92 \pm 3	100 \pm 6	103 \pm 4	105 \pm 6	99 \pm 4	118 \pm 5

4. DISCUSSION

SPS of atomized powders resulted in a full densification with minimized influence on powders microstructure. The direct heating during SPS led to partial dissolution of continuous layers of intermetallic particles present in the atomized powder particles. Because of the short thermal exposure, the solute atoms cannot diffuse over a large distance. During cooling from the SPS temperature the precipitates were reformed at the former boundaries of dendrites or cells, which are preferential sites for heterogeneous nucleation.

The high energy ball milling or cryomilling introduced high deformation energy into the material due to collisions of balls and powder particles, which also led to repeated fraction and cold welding of the powder [2]. This process resulted in an increased microstrain. The microhardness increase with increasing intensity of milling can be explained predominantly by increased density of dislocations. Simultaneously, most relatively coarse particles of intermetallic phases were destroyed during milling and solute atoms contribute to microhardness by solid solution strengthening. According to [9] Mg is able to form MgO oxide phase by deoxidizing the amorphous Al₂O₃ surface layer of particles. During milling the surface oxide can be introduced into material and result in oxide dispersion strengthening [2]. The high standard deviation of HV in powder materials reflects the heterogeneity of powder particles microstructure as each indent was applied in another powder particle.

During SPS the temperature of sintering was set to 425 °C and even much higher temperature can be expected at contact points of powder particles. XRD revealed an increase in crystallite size and a decrease in microstrain in compacts of milled powders which can be explained by recrystallization process. This is confirmed by EBSD measurement showing a bimodal microstructure with a large fraction of submicrometer grains and bands of larger grains up to 5 μm. This heterogeneity in grain size of SPS compacts from milled powders could be caused by non-uniform distribution of deformation introduced during milling [10]. Similar microstructures were presented in several other studies [11-13]. Zuniga et al. [11] claimed that the coarse grains could be formed due to localized high temperatures at the beginning of the SPS process, since before densification, the current flows through a very limited number of contact points of powder particles. It was shown in [12] that the coarse grains have no preferred orientation, therefore their growth is not influenced by the applied pressure direction, showing, that SPS led to random orientation of new grains. Similar bimodal grain structure was also found in steel [13], where it was explained by non-homogeneous distribution of nanoprecipitates leading to abnormal grain growth of some grains due to unpinned boundaries. In our case the EBSD map shows curved bands of coarse grains neighboured by curved bands of finer grains. This microstructure seems to stem from the milling process, where powder particles flattered by collision were cold welded together. During SPS these cold welded particles recrystallized in a heterogeneous manner due to a different stored deformation at different places.

During SPS of milled powders the remaining not dissolved precipitates coarsen and new ones are formed from the supersaturated solid solution. Due to the high dislocation density inside the powders the diffusion process is enhanced leading to fast formation of new phases. The heterogeneity in intermetallic particle distribution vanishes with increasing intensity of milling since intensive milling led to an increase in homogeneity of introduced deformation, solute atom and precipitate distribution. The decrease in milling temperature has no significant influence, neither on microstructure nor on microhardness of SPS compacts. The precipitation of relatively coarse particles and recrystallization reducing dislocation density result in a decrease of HV in all SPS compacts.

5. RESULTS

The Al7075 alloy prepared by spark plasma sintering of atomized, milled and cryomilled powders was studied. Milling process destroyed most intermetallic particles and resulted in a significant hardening through dislocation, solid solution and dispersion strengthening. SPS process led to dense compacts. In initially atomized powders a negligible effect of SPS on microstructure was found. SPS of milled powders led to

recrystallization resulting in a bimodal fine-grained structure and to a heterogeneous distribution of precipitates. Both processes are responsible for a decrease in microhardness.

ACKNOWLEDGEMENTS

This work was financially supported by the grant GACR 15-15609S.

O.M. is grateful for financial support from the grant SVV-2016-260213 and acknowledges the support from the Grant Agency of Charles University under contract Nr. 1882314.

REFERENCES

- [1] HUANG, Y., LANGDON, T.G. Advances in ultrafine-grained materials. *Materials Today*, 2013, vol. 16, no. 3, pp. 85-93.
- [2] SURYANARAYANA, C. Mechanical alloying and milling. *Progress in Materials Science*, 2001, vol. 46, no. 1-2, pp. 1-184.
- [3] PICKENS, J.R. Aluminum powder metallurgy technology for high-strength applications. *Journal of Materials Science*, 1981, vol. 16, no. 6, pp. 1437-1457.
- [4] GUPTA, M., MOHAMED, F., LAVERNIA, E. J. Solidification characteristics of atomized AlTi powders. *Scripta Metallurgica et Materialia*, 1992, vol. 26, no. 5, pp. 697-702.
- [5] SUAREZ, M., FERNANDEZ, A., MENENDEZ, J. L., TORRECILLAS, R., KESSEL, H. U., HENNICKE, J., KIRCHNER, R., KESSEL, T. Challenges and opportunities for spark plasma sintering: A key technology for a new generation of materials. In *Sintering Applications*, InTech, 2013, pp. 319-342.
- [6] RIETVELD, H. M. Line profiles of neutron powder-diffraction peaks for structure refinement. *Acta Crystallographica*, 1967, vol. 22, no. 1, pp. 151-152.
- [7] HILL, R.J., HOWARD, C. J. Quantitative phase analysis from neutron powder diffraction data using the Rietveld method. *Journal of Applied Crystallography*, 1987, vol. 20, no. 6, pp. 467-474.
- [8] MOLNÁROVÁ, O., MÁLEK, P., BECKER, H. The investigation of the Al7075 + 1 wt % Zr alloy prepared using spark plasma sintering technology. In *METAL 2015: 24th International Conference on Metallurgy and Materials*, Brno: TANGER, 2015, pp. 1221-1226.
- [9] XIE, G., OHASHI, O., SATO, T., YAMAGUCHI, N., SONG, M., MITSUISHI, K., FURUYA, K., Effect of Mg on the sintering of Al-Mg alloy powders by pulse electric-current sintering process. *Materials Transactions*, 2004, vol. 45, no. 3, pp. 904-909.
- [10] LIAO, X. Z., HUANG, J. Y., ZHU Y. T., ZHOU, F., LAVERNIA, E.J. Deformation mechanisms at different grain sizes in a cryogenically ball-milled Al-Mg alloy. In *Ultrafine Grained Materials II*, John Wiley & Sons, Inc., Hoboken, NJ, USA, 2002, pp. 323-330.
- [11] ZUNIGA, A., AJDELSZTEJN, L., LAVERNIA, E.J. Spark plasma sintering of a nanocrystalline Al-Cu-Mg-Fe-Ni-Sc alloy. *Metallurgical and Materials Transactions A*, 2006, vol. 37A, pp. 1343-1352.
- [12] KUBOTA, M., WYNNE, B.P. Electron backscattering diffraction analysis of mechanically milled and spark plasma sintered pure aluminum. *Scripta Materialia*, 2007, vol. 57, no. 8, pp. 719-722.
- [13] ZHANG, H., HUANG, Y., NING, H., WILLIAMS, C.A., LONDON, A. J., DAWSON, K., HONG, Z., GORLEY, M.J., GROVENOR, Ch.R.M., TATLOCK, G.J., ROBERTS, S.G., REECE, M.J., YAN, H., GRANT, P.S. Processing and microstructure characterisation of oxide dispersion strengthened Fe-14Cr-0.4Ti-0.25Y2O3 ferritic steels fabricated by spark plasma sintering. *Journal of Nuclear Materials*, 2015, vol. 464, pp. 61-68.